Advances in indoor location

F. Barceló, Technical University of Catalonia (UPC)
F. Evennou, France Telecom R&D
Luca de Nardis, University of Rome La Sapienza
Phillip Tome, Swiss Federal Institute of Technology

***Abstract*— This paper presents the research activities carried out within the scope of the Liaison project. Most of the work has been performed on WiFi location. WiFi is nowadays widely deployed in buildings such as hotels, hospitals, airports, train stations, public buildings, etc. Using this infrastructure to locate terminals connected to the wireless LAN is expected to have a low cost. Methods presented in this paper include fingerprinting and tracking through particle filter constrained on a Voronoi diagram and TOA based on data frames and acknowledgments at the link level. Other technologies have also been researched: A-GNSS to handle the transition between outdoors and indoors, UWB in ad-hoc mode to cope with possible lacks of infrastructure and inertial MEMS to increase the availability and robustness of the overall system.**

I. INTRODUCTION

A. Location Based Services

Recently, there has been a growing interest on location-based services (LBS). LBS are addressed particularly to mobile networks. They can be defined as services that adapt to a user's location and situation: location is a crucial input for these applications. LBS explore the ability of technology to know where the user is and shape the information provided accordingly.

Presently, many LBS have already been deployed and others that have been designed are ready for commercial implementation. A few of the most interesting ones are described below.

- Information services.
- Navigation.
- Workforce management
- Lone worker applications
- Children tracking.
- Medical alert.

Location services can be classified according to technical parameters. In the case of LBS, QoS parameters are usually proposed. Several parameters may be used to measure QoS in a LBS. The 3GPP proposes quantifying QoS according to two parameters: minimum accuracy and maximum response time. Minimum accuracy refers to the maximum error that the LBS supports. Usually, customer position is delivered to the location client as a information pair: position and location area. The position represents the estimated position, while the location area sets the boundaries of possible error range. Maximum response time is defined as the maximum time that the LBS takes until its completion. These two parameters are included in all QoS definitions for LBS. However, several parameters may be added, depending on the scenario. For instance, availability indicates the coverage expected by the user, i.e. the percentage of time and space in which the LBS is operative.

B. Indoor location

Outdoors is the typical scenario for GPS positioning and tracking. When the terminal to be located has an open view of the sky, GPS is expected to give good or even excellent accuracy. Difficulties with GPS positioning usually occur in urban canyons and indoors, where it is difficult or impossible to acquire the necessary satellites for a position computation. Recently, research has been intensified on location systems that use the cellular network to provide the terminal's position. Both GSM and UMTS allow positioning with good or excellent accuracy with the only requirement of a good number of base stations at sight. This is actually the case in urban canyons, since urban areas are typically well covered by cellular networks. Also in light indoors (e.g. close to windows) a good accuracy can be provided. But, when the terminal to be located goes several meters indoors or is surrounded by obstacles, such as walls, penetration of the signals coming from several base stations is difficult due to attenuation. Problems are found in medium to deep indoors, electrically noisy indoor scenarios, subterranean places (e.g. parking), and others.

II. FINGERPRINTING IN WLAN

Many outdoor systems are based on time measurements. Thus, the mobile can calculate the distance separating him from the base stations or satellites.

However getting this kind of information with off-the-shelf WiFi equipments is almost impossible. The only available information is the signal strength received from each access point (AP). Indeed, the received signal strength is measured and is one of the outputs of the card. Such information is available because the APs send beacons periodically. Mobile devices use those beacons to handle the roaming inside the network. Given this consideration, it is possible to get a list of the received power coming from all the APs covering the area where the mobile is moving.

A. WiFi Cell ID, signal strength and fingerprinting

The simplest approach for locating a mobile device in a WLAN environment is to approximate its position by the position of the access point received at that position with the strongest signal strength. The major benefit of such a system is its simplicity, but its main drawback is its large estimation error. The accuracy is proportional to the range of access points which is within 25 and 50 meters for indoor environments [10]. Using a propagation model [8][9] to turn RSS measurements into distances, did not provide satisfying results when these range were introduced in a multilateration algorithm. [11] introduces a different approach for locating the device in indoor environments by using the radio signal strength fingerprinting.

Fingerprinting positioning is a quite different technique. It consists in having some signal power footprints or signatures that define a position in the environment. This signature is made of the received signal powers from different access points that cover the environment. A first step, called training for profiling, is necessary to build this mapping between collected received signal strength and certain positions in the building. This leads to a database that is used during the positioning phase. Building the footprint database can be done in two ways. A first method is to do on-site measurements for some reference positions in the building with a user terminal. An alternative approach is based on collecting limited on-site measurements and introducing them in a tunable propagation model that would use them to fit some of its parameters. Then, this propagation model gives an extensive coverage map for each AP. However, the poor results obtained earlier with the use of the propagation model, did not invite us to focus on such a model. Neural networks are another learning method for improving propagation models over time [12]. It was decided to carry on with the use of the data collected to build the database. Ray tracing tools represent another solution to build such a database, but they are very complex tools. Moreover, a good knowledge of the radio environment (knowledge of the presence and position of all the APs is needed) to cope with the interfering issue. However, such information is not always available due to the fast growing emergence of this technology in indoor environments.

Once this prerequisite step is accomplished, it is necessary to do the reversing operation, which will deliver the position associated to an instantaneous collected tuple of received signal strengths. Different techniques can fit these requirements.

1) k-closest neighbors fingerprinting: This algorithm goes through the database and picks the k referenced positions that match the best the observed received signal strength tuple. The criterion that is commonly retained is the Euclidian distance (in signal space) metric. If $Z=[RSS_1,\cdots,RSS_M]$ is the observed RSS vector composed of M received access points at the unknown position $X=(x,y)$ and Z_i the footprint recorded in the database for the position $X_i=(x_i,y_i)$ then this Euclidian distance is

$$d(Z,Z_i)=\frac{1}{M}\cdot\sqrt{\sum_{j=1}^{M}\left(RSS_j(x,y)-RSS_j(x_i,y_i)\right)^2}$$

where $RSS_j(x_i,y_i)$ is the mean value recorded in the database for the access point whose MAC Address is noted " j " at the position (x_i,y_i).

The set N_k of the database positions having the smallest errors is built with an iterative process as follows:

$$N_k=\left\{\underset{X_i\in\Im}{\operatorname{argmin}}\left[d(Z,Z_i)\right]\setminus X_i\notin N_{k-1}\right\}$$

where $\Im$ is the set of positions recorded in the database.

This set contains k positions. Finally, the position of the mobile is considered to be the barycenter of those k selected positions.

$$X=\frac{\sum_{j=1}^{k}\frac{1}{d(Z,Z_i)}\cdot X_j}{\sum_{j=1}^{k}\frac{1}{d(Z,Z_i)}}\quad\text{with } X_j\in N_k$$

The main advantage of this method is its simplicity to set it up. However the accuracy highly depends on the granularity of the reference database [13]. A better accuracy can be achieved with finer grids, but a finer grid means a larger database what is more time-costly.

However, the signal strength fluctuations (Figure 1) introduce many unexpected jumps in the final trajectory.

Removing those jumps can be done by using a filter. Kalman filter and particle filter are often used in parameter estimating problems and tracking. This last filter will be introduced in the next section, and the benefits using such a filter will be presented.

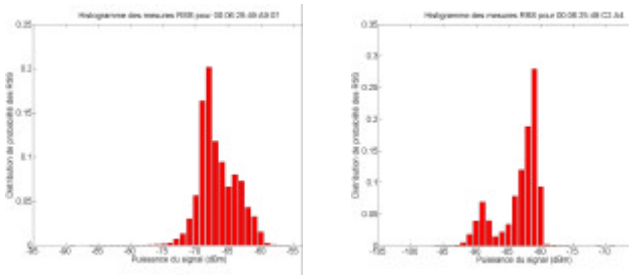

Figure 1: Signal strength variations over the time, for the same position (examples given for two different access points)

B. Improving WiFi positioning with a particle filter constrained on a Voronoi diagram

Nowadays, the maps of all the public or company buildings are available in digital format (dxf, jpeg, etc). The key idea is to combine the motion model of a person and the map information in a filter in order to obtain a more realistic trajectory and a smaller error for a trip around the building. In the following, it will be considered that the map, which is

available, is a bitmap. So no information is available except the pixels in black and white which model the structure of the building. The particle filter, based on a set of random weighted samples (i.e. the particles), represents the density function of the mobile-position. Each particle explores the environment according to the motion model and map-information. Their weights are updated each time a new measurement is received. However the free particle filter is not fit handset based applications, as the computations are quite heavy. At each time step, it is necessary to check if a particle crossed a wall or not in order to introduce the architecture of the building in the filter. An approach to reduce this computation complexity is to limit the space the particles need to explore. Another representation for the building is a graph. These sets of edges and nodes make the skeleton of the building. Constraining the particles to move of this representation of the building is really interesting, as it is not necessary to check if particles crossed a wall or not.

The particle filter tries to estimate the probability distribution $\Pr\left[X_k \middle| Z_{0:k}\right]$ where X_k is the state vector of the device at the time step k, and $Z_{0:k}$ is the set of collected measurements until the $(k+1)^{th}$ measurement. When the number of particles $\left(\text{positions } x_k^i, \text{ weight } w_k^i\right)$ is high, the discrete probability density function of presence can be assimilated to:

$$\Pr\left[X_k \middle| Z_{0:k}\right] = \sum_{i=1}^{N_s} w_k^i \cdot d\left(X_k - X_k^i\right)$$

This filter comprises two steps:

- Prediction
- Correction

1) The Voronoi diagram

The Voronoi diagram [16] has been used for a long time in the robotics community to model the environment in which a device is evolving. The Voronoi diagram is a set of edges that are equidistant to all the walls. This space is represented by:

$$V = \left\{x \in W \setminus \left(C_i \cup C_j\right) \quad d_h(x) \geq d_i(x) = d_j(x) \geq 0\right\}$$

with i, j, h three objects present in the environment (walls for example).

The first stage was to automatically design this Voronoi diagram from a bitmap picture. A routine has been done to achieve this task (Figure 2).

With such a representation, it is possible to limit the moves of the particles. Now they are constrained to move on the edges of the oriented graph. This reduces the processing cost at each time step. There is no need to check if a particle crossed a wall or not. As they have a reduced area to explore, it is possible to cut down the number of particles. In our simulations, only 200 particles were used to track the device. Indeed, the particles move in a graph which is a one dimensional space whereas in the previous case, the particles were moving in a two dimensional space.

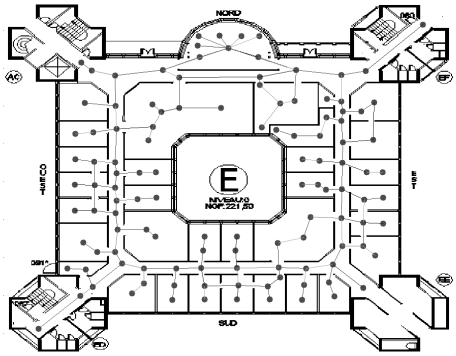

Figure 2: Voronoi diagram for a building (set of edges and nodes)

2) Prediction

During this step, the particles propagate across the building given an evolution law that assigns a new position for each particle with an acceleration governed by a random process:

$$\begin{bmatrix} d_{k+1}^j \\ v_{k+1} \end{bmatrix} = \begin{bmatrix} 1 & T_s \\ 0 & 1 \end{bmatrix} \cdot \begin{bmatrix} d_k^i \\ v_k \end{bmatrix} + \begin{bmatrix} \frac{T_s^2}{2} & 0 \\ 0 & T_s \end{bmatrix} \cdot m_k$$

where $\begin{bmatrix} d_k^i & v_k \end{bmatrix}^t$ denotes the state vector associated to each particle (position on the edge i and speed), T_s the elapsed time between the $(k+1)^{th}$ and the k^{th} measurements. m_k is a random process that simulates the acceleration of the k^{th} particle. This last equation is often called the prior equation. It tries to predict a new position for all the particles. Here the used process is a zero mean Gaussian noise with a $0.1\, m/s^2$ variance which is a realistic model of pedestrian movement. Here we must handle the transition between edges, because the particle can go from one edge to the other over the time. Moreover, after the observation of the moves of a pedestrian, we can see that most of his movements are in straight line. This observation can be introduced in the filter when handling the transitions of the particles from one edge to another. A good way to take this piece of information into account is to introduce it in the particle filter with the pdf $\Pr\left[X_{k+1} \middle| X_k\right]$. When a mobile changes the edge on which it is, it must choose one among the next ones. It can be chosen randomly. If all the edges have the same probability, any of the next edges can be chosen as the next one without any preference. However, in our motion model when a person faces an intersection this is not true. Then, to choose the next edge with a probability, we retained the following heuristic criterion:

$$\Pr\left[V_k\right] = \frac{1+\cos q_{j,k}}{\sum_m \left(1+\cos q_{j,m}\right)}.$$

with $q_{j,k}$ the angle between the edges V_j and V_k. Here the particle is considered to be on the edge V_j.

If the speed of the particle is positive, m is the index of the edges that have in common the ending node of V_j, otherwise they have in common the starting node of V_j. Then, the next edge on which the particle will move is drawn according to the law defined above.

3) Correction

When a measurement (n-uplet of RSS) is available, it must be taken into account to correct the weight of the particles in order to approximate $\Pr\left[X_k \middle| Z_{0:k}\right]$. As the measurement is signal strength and given that particles are characterized by their position, the RSS n-uplet must be transformed into a position. The mapping between the position and the signal strength is performed thanks to the empirical database. In fact, the algorithm used in section II to find the position of the mobile given the RSS coverage in the building is used. Then it is possible to estimate $\Pr\left[Z_k \middle| X_k\right]$. In the case of an indoor movement, the following law has been retained:

$$\Pr\left[Z_k \middle| X_k\right] = \frac{1}{\sqrt{2p}\,s}\exp\left[-\frac{\left(X_{Z_k} - X_k\right)^2}{2\cdot s^2}\right]$$

with X_{Z_k} the position returned by the database, X_k the position of the k^{th} particle and s the measurement confidence. The smaller s will be, the more confident the user is in the measurement. That would mean that there is very little variations in the measurements for the same position. Here, given the variations of the RSS, $s = 5m$ was chosen. It can be noticed that with this gaussian law, the closer the particle is to the position returned by the database, the higher its $\Pr\left[Z_k \middle| X_k\right]$ will be. Now, we have defined all the necessary probabilities to update the weight of a particle, we just need to combine them to find the new posterior distribution.

4) Update of the weights

The weight update equation is given in [11][12]:

$$w_k^i = w_{k-1}^i \cdot \Pr\left[X_k \middle| X_{k-1}\right] \cdot \Pr\left[Z_k \middle| X_k\right]$$

To obtain the posterior density function, it is necessary to normalize those weights. After a few iterations, when too many particles crossed a wall, just a few particles will be kept alive (particles with a non zero weight). To avoid having just one remaining particle, a re-sampling step is triggered.

5) Resampling

The re-sampling step is a critical point for the filter. The basic idea behind the re-sampling step is to move the particles that have a too low weight, in the area of the map where the highest weights are. This leads to a loss of diversity because many samples will be repeated. The criterion to trigger a resampling is given by:

$$\frac{1}{\sum_{i=1}^{N_s}\left(w_k^i\right)^2} \le Threshold$$

Various resampling algorithms are proposed in [19]. We chose the simple SIS (Sequential Importance Sampling strategy) algorithm for its simplicity and low complexity order. The complexity must be taken into account as the algorithm must run on a handheld device which can have low processing capabilities.

C. Experiments

To experiment with all those techniques and estimate their capabilities and accuracy to localize a device, a demonstrator has been built. It is made of a set of four 802.11g Linksys WAP54g APs placed at each corner of the 35×35 m building. The mobile device (PDA) is evolving in an indoor office environment. Both, a laptop and a Compaq iPAQ 4700 PDA were used for the measurements.

The database is built with one measurement in each room, and a measurement every two meters in the corridor. The single floor problem is considered. The criterion to define the error is the mean error over a trip in the building ($\bar{e}(m)$ in meters). A walk around the building is taken for the test. Some real measurements are collected along this path and then reused to estimate the performances of this positioning technique based on WiFi. Here the measurement frequency is $3.33\,Hz$ and the handheld device computes itself his own position.

One of the parameters that influences the performances of the positioning system, is the number of access points. With the fingerptrinting technique, it is not necessary to know the position of the access points to estimate the position of the mobile. Here we have 4 access points with a known position, and then multiple other access points with an unknown position in the building. A first study on the influence of this parameter has been carried out. Figure 3 presents the instantaneous errors over 100 simulations with different access points chosen for each simulations.

These curves shows that having many access points is useful as the more there are access points in a footprint, the easier it is to get the closest footprint to the instantaneous measurement. However, getting a realistic estimate of the trajectory with the closest neighbour algorithm is not satisfying.

Using the fingerprinting shows that it is not possible to recognize the path followed by the mobile moving across the building. All the positions referenced in the database have been selected over the time. It is necessary to filter information over the time to be able to obtain a coherent trajectory. Here results for two trajectories are presented. One of these trajectories remains in the corridor whereas during the second one, the mobile enters a room.

For this trajectory, the 4 access points under our control were used. The particle filter runs with 200 particles. In each situation, we see that the estimated trajectory fits the real one. Large errors appear at the beginning, because we suppose that the filter does not know were the mobile is standing. Particles are disseminated all over the building. After some few time steps, the filter starts tracking the device correctly.

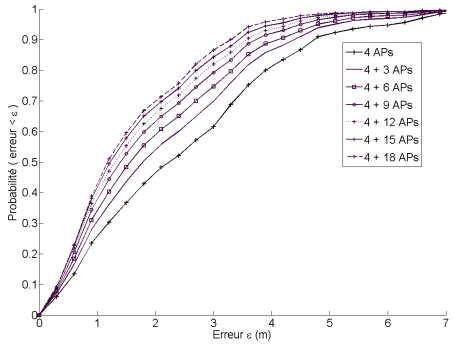

Figure 3: Influence of the number of access points on the fingerprinting technique

.

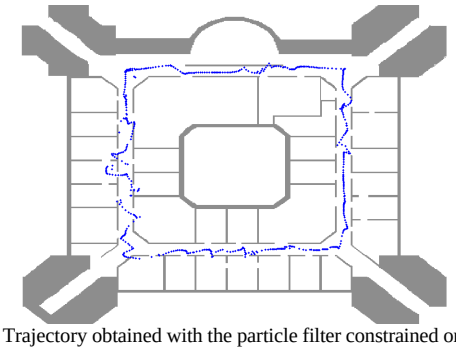

Figure 4 : Trajectory obtained with the particle filter constrained on a Voronoi diagram

Table 1 shows that it is possible to have a 2 m accuracy with a WiFi positioning system, with a low infrastructure. Increasing the density of access points improves the performances, however such deployment does not appear to be realistic. The filter also improves the trajectory estimated for the mobile. It is possible to have a clear idea of the places where it went. When it stops in a room, the estimated positions fluctuate in that room. Here, WiFi cannot provide information to the filter that the mobile stopped. Using extra sensors is required, like MEMS sensors (used in the inertial navigation systems). Moreover, the filter presented here can be implemented on handheld devices, and can run on them. The computation times for different filters are presented in Table 2. [18] presents a comparison between these different filters. The particle filter constrained on a Voronoi diagram appears being a good trade off between complexity (computation time of a measurement) and performances, as the performances of this filter are similar to the one achieved with the particle filter with particles freely moving.

Table 1: Performances of the algorithm (traj1: Trajectory in the corridor, traj2: Trajectory in the corridor + stop in a room)

	4 APs		22 APs	
	67%	95%	67%	95%
Error (m) traj 1	1.92	3.31	1.20	2.24
Error (m) traj 2	2.6	4.57	2.11	3.95

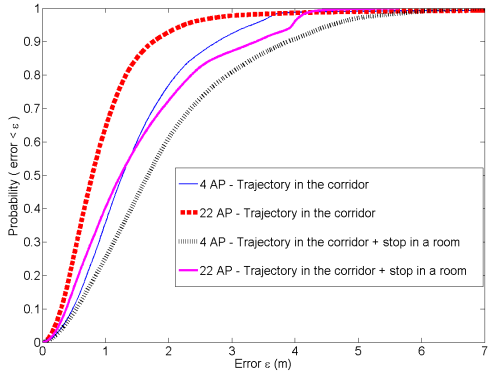

Figure 5: Cumulative distribution function of the instantaneous errors over 100 simulation of the same trajectory.

Table 2: Computation time (in ms) for a RSS n-uplet with a laptop (GHZ processor, 1024 Mo RAM) and a PPC (Hp4700, Proc 624 MHz, 64 Mo SDRAM)

	Percentage of time	50%	67%	75%	90%	95%
PC	Fingerprinting	3	3	3	4	4
	Particle filter	10	13	13	16	17
	Particle filter + Voronoi	3	4	4	5	6
PPC	Fingerprinting	5	5	5	6	6
	Particle filter	373	567	600	673	714
	Particle filter + Voronoi	8	8	8	9	12

III. TOA WITH DATA LINK FRAMES

A. *Introduction*

The research challenge corresponds to achieve an indoor location system capable to provide accurate positioning using the existing WLAN infrastructure and devices with minor changes, avoiding the need of synchronization between access points (APs) and long manual system pre-calibrations (i.e. build of fingerprinting database), while presenting robustness to environmental changes (i.e. furniture). Following this direction, here it is presented a new indoor WLAN location technique based on distance measurements provided by TOA estimations—which are in turn based on round-trip time (*RTT)* measurements at IEEE 802.11 link layer—between the mobile terminal (MT) to be located and WLAN APs. The system is divided into the ranging and the positioning subsystem. The former estimates the distances between the MT and the APs, and the latter calculates the MT position using the distances and the APs' known positions. One challenge corresponds to achieving accurate estimations from *RTT* measurements performed using a standard IEEE 802.11b card clock at 44 MHz, which shall lead theoretically to errors of 7 m.

Several contributions existed in the scope of the proposed system, but none of them fulfilled the degree of desired accuracy, simplicity and flexibility. In [1], a new approach is proposed to ranging in IEEE 802.11, without the requirement of initial synchronization between transmitters and receivers. Ranging is achieved by using a high precision timer in order

to measure TDOA from two GRP (Geolocation Reference Point). The authors also propose to take advantage of the IEEE 802.11 data link frames for measuring TOA (time-of-arrival), but they do not give more insight to this matter. In [2], a system which can estimate TOA using IEEE 802.11 link layer frames is proposed, but the RTS (Request-to-Send)/CTS (Clear-to-Send) mechanism is required. Their ranging technique relies on internal delay calibration both at transmitter and receiver in order to correct the round-trip time (*RTT*). To mitigate multipath impact, the authors propose to use different carrier frequencies and to discriminate between strong and weak multipath (i.e. greater than three chips from the direct path) in order to apply different curve-fitting algorithms and obtain 1m or 3m accuracy. In [3], a method to estimate TOA between WLAN nodes without using extra hardware is presented, but the achieved accuracy (error of 8 meters) is not enough for some safety applications.

B. Ranging system

1) RTT estimation

a) Approach

Round-trip time is the time a signal takes to travel from a transmitter to a receiver and back again, in our case from a MT to a fixed AP. As can be seen in Fig.6, we estimate the *RTT* by measuring the time elapsed between two consecutive frames under the IEEE 802.11 standard: a link layer data frame sent by the transmitter (it is the MT) and the reception of the correspondent link layer acknowledgement (ACK) from the receiver (it is the AP). Other link layer frames would be also suitable [2].

The MT is a laptop with an IEEE 802.11b PCMCIA card. As the overall (i.e. propagation plus processing) *RTT* is expected to be in the order of microseconds, measuring it with software as in [3] leads to a significant lack of accuracy. Therefore, we propose to measure the *RTT* through a simple hardware module that starts counting cycles of the built-in 44 Mhz clock from the WLAN card when it detects the end of transmission of a data frame, and it stops when the corresponding ACK frame arrives**.** Then it sends its value (i.e. slotted in 44 MHz periods) to the laptop PC.

b) Mitigation of errors

It should be possible to estimate a distance by using only one *RTT* measurement. However, the *RTT* is time-variant due to constraints such as the variability of the radio channel multipath [4], the 44 MHz clock quantification errors [3], delays due to the electronics of the hardware module and the relative clock drift. If we only considered the quantification errors, a distance estimation error of 7 m should be present. In order to mitigate these errors this paper proposes to perform several (*n*) *RTT* measurements and to use a proper *RTT* estimator based on the statistical set obtained.

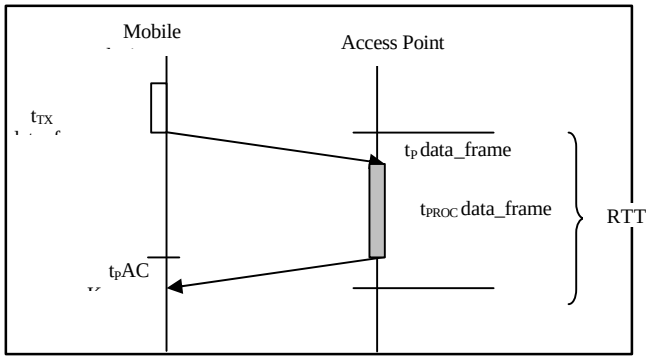

Figure 6. *RTT* measurement using IEEE 802.11 data/ACK frames

First, it was verified that every obtained *RTT* was independent and not correlated with the rest of them. Hence, the autocorrelation function for several series of 1000 *RTT* samples -corresponding to different real distances between the MT and the AP- were obtained. All of them showed negligible correlation.

The chosen *RTT* estimator was the average *RTT* value (*h*, measured in number of clock cycles) obtained from all the measurements, since among all tested choices this value provided the best *RTT* estimation. Other choices, such as the half range *RTT*, the *RTT* mode, the average of *n* minimum *RTT* values and *h- b* times the standard deviation were also tested but they did not provide the best accuracy and are not reported in this paper.

c) Number of RTT measurements needed

The number of *RTT* measurements needed to estimate the *RTT* is relevant in order to find a reasonable trade-off between bandwidth used, time employed and accuracy obtained. Since *RTT* is a random variable and the average is used as estimator, the number of *RTT* samples can be set from a target confidence interval of the estimated average –around the population average- for a certain confidence level (95% of the time). Hence, the number of required samples is:

$$n = (2 \cdot z_{0.975} \cdot S / A)^2, \quad (1)$$

where *S* the estimated standard deviation, $z_{0.975}$ the *z* function value for a confidence level of 95% and *A* is the width of the confidence interval. Taking into account that every 44 MHz rising clock implies a distance of 7 m., it was considered that only values of *A* under 0.5 (it is 0.25 rising clocks around the population average) had to be accepted. It was obtained *n* = 246; being aware that usually a small portion of the performed *RTT* measurements are not valid (due to errors of several types), *n* = 300 seemed to be a conservative figure to accurately estimate the *RTT*.

2) Distance estimation

a) Method

First, a *RTT* estimation at zero distance between the MT and the AP is obtained (the propagation times t_p is zero), in order to calibrate the time the AP takes to process the query

(i.e. the link layer processing time). The figure obtained is assumed to be the t_{proc} *data_frame* part in Fig. 6 so that it can be used as an offset for measurements at a non-zero distance. Consequently, by applying the offset obtained, it is possible to find the ΔRTT , it is the pure propagation time of the *RTT*:

$$\Delta RTT = RTT_a - RTT_0 . \quad (2)$$

Once the ΔRTT is calculated -and being aware that a 44 MHz clock was used for the measurements- the distance d (in meters) between the transmitter and receiver can be obtained as

$$d = c \cdot t_p = c \cdot \left(\Delta RTT / 2 \cdot 44 \cdot 10^6 \right) . \quad (3)$$

Taking into account that the *RTT* estimator is the average *RTT* value (h, measured in number of clock cycles), Eq. (3) can be rewritten as:

$$d = ((h_a - h_0) \cdot 3 \cdot 10^8)/(2 \cdot 44 \cdot 10^6). \quad (4)$$

b) Empirical coefficient

During the development process, it was observed that all the distances estimated were longer than the actual distances; therefore, the estimated distance had to be divided by an empirical coefficient to correct the estimated value. This coefficient is justified by the special characteristics of the multipath indoor radio propagation channel [5], the measurement quantification errors and the delays caused by the electronics of the hardware module, which can increase the theoretical expected *RTT*.

To estimate that coefficient all *RTT* measurements were analyzed and gathered according to the specific distances they belong. Afterwards, linear regression lines were traced relating the estimated distance obtained following the method described above with the actual distance (i.e. straight lines and not exponential or logarithmic relationship appeared between both variables). Furthermore, this relation did not show any independent term. The result is shown in Fig. 7, being k=0.694 the coefficient found.

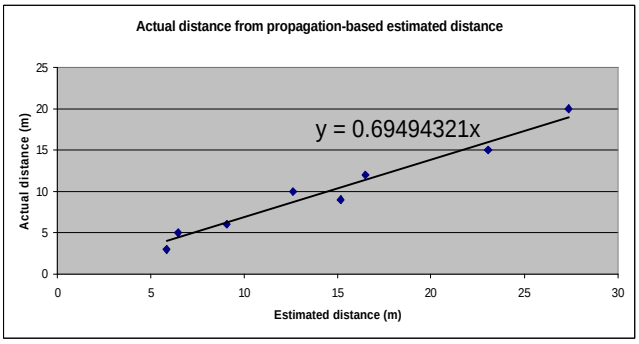

Figure 7. Estimation of the empirical coefficient

Therefore the corrected formula for calculating the distance is:

$$d = ((h_a - h_0) \cdot 3 \cdot 10^8 \cdot k)/(2 \cdot 44 \cdot 10^6). \quad (5)$$

3) Experimental Test Bed and Measurements

The experimental test bed consists of several distance estimations in the laboratory and its surroundings, under different conditions and with varying numbers of people in the rooms, at different times of the day, at various temperatures, and under different weather conditions. Therefore, all the measurements were taken in a real indoor working environment and without differentiating between LOS and NLOS situations. The accuracy of the ranging system was studied by performing several range estimations at different distances. Table 3 shows the absolute and relative errors obtained for every distance.

Table 3. Results of the ranging subsystem

Distance	**5 m**	**10 m**	**15 m**	**20 m**
Average	0.51 m (10.2%)	0.51 m (5.1%)	1.38 m (9.2%)	0.47 m (2.3%)
Maximum	1.21 m (24.2%)	1.24 m (12.4%)	2.88 m (19.2%)	1.01 m (5.0%)

In a second set of measurements, the probability distribution of the distances estimated by the ranging system was obtained. One of the objectives of this statistical characterization is to feed the positioning subsystem simulations with actual distance measurements, as below discussed in Section III.C.3 This set of measurements consists of 450 distance estimations (450*300 *RTT* measurements), measured at a constant distance of 10 m, after the initial calibration at 0 m.

Ideally, all the distances measured should be 10 m; however, due to several error sources, the ranging system obtains distances from 8.80 m to 12.80 m. This empirical histogram was compared with known probability distributions. The best fit was found to be a Gaussian distribution, as can be seen in Fig. 8, with $m = actual\_dist + 1.12$ and $s = 0.84$.

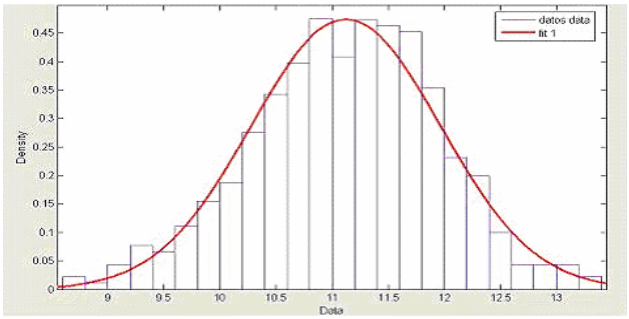

Figure 8. Histogram of distance measurements

C. Positioning System

1) Introduction

The MT position can be estimated once the distance

estimations from a set of AP are obtained and the APs coordinates are known. The simplest option is to use a pure triangulation algorithm but higher accuracy can be achieved if tracking is applied, because it takes advantage of the past trajectory followed by the MT. Specifically, a Kalman-based tracking algorithm has been designed due to its simplicity and potential performance features. For a detailed description of the Kalman filter see [6] and [7].

The main idea of the Kalman filter is to perform a weighted average estimation process in two steps: first the filter estimates the current position from past ones (time update or prediction step) and second it obtains the feedback from the noisy measurements –it is the distance estimations- in order to improve the accuracy of the estimation (measurement update or correction step). The weight of every source of information depends on the reliability that can be assumed for each one, expressed in terms of noise covariance matrix figures.

2) Customized Kalman-based algorithm

The MT's motion model assumed by the filter is defined in the prediction step. It was decided to optimize this part of the filter in order to maximize the accuracy. The new approach relies on supposing that the target is going to follow the straight trajectory defined by the line that joins the last two estimated positions, with the same speed and direction. Hence, in practice, the position can be predicted following basic geometrical laws. The speed of the target is estimated from the last past five estimated positions.

3) Experimental Test Bed: Simulations

Simulations have been carried out in order to evaluate the performance of the positioning system using the Kalman-based described approach. Furthermore, the Non Linear Least Squares (Newton) trilateration algorithm has also been implemented in order to evaluate the advantage of tracking results versus pure positioning techniques. For this evaluation it was desired to obtain the Cumulative Distribution Function (CDF) of the absolute positioning error.

The observables that feed the filter (i.e. in the correction step) on every position estimate correspond to the distance estimations from the MT to the three nearest APs, using the actual ranging results presented in Section III.B.3. In practice, every observable is obtained by calculating a single random value from a normal random variable with the above mentioned parameters. Thus it is essential to perform a large number of runs of a specific route simulation in order to guarantee that the actual ranging model is really used. This way the results of these simulations are fair and theoretically almost the same as the ones obtained with a tracking prototype in an actual indoor environment.

A large number of routes (5000) with bad GDOP zones and probable changes of direction were generated following a motion model as similar as possible to a real behavior of a pedestrian. The motion algorithm is managed by the following rules:

- The probability of changing the direction at a given time is governed by a geometrical random distribution. with probability of change = 0.1. Hence, the average number of time units following the same direction is 10.
- The speed of the MT is a normal random variable of mean 1 m/s and variance 0.2 m/s. The speed is allowed to vary only when the direction changes.
- The change of direction can be up to 30 degrees respect the followed straight line.

The scenario is composed by a squared area of 50x50 m^2 with an AP in every corner. The positioning step T is set to 1 second.

4) Results

Fig. 9 shows the CDF of the absolute positioning error for the algorithms. It can be seen that the Kalman-based algorithm provides a high accuracy of less than 0.9m. of absolute positioning error for the 66% of the cases (one sigma), and less than 1.4m. for the 90%. Comparing it with Newton, the improvement seems to be noticeable, because it provides 1.8m. and 1.2m. for the 90% and the 66% respectively.

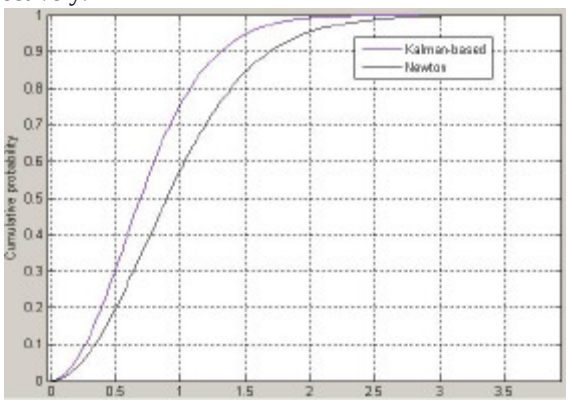

Figure 9. CDF of the absolute positioning error

Fig. 10 shows an interval of one of the generated MT's trajectory and the estimated ones obtained with Newton and the Kalman-based algorithms. It can be easily appreciated that the later provides an erratic path whereas the former is able to achieve a smoothed trajectory very similar to the actual one.

D. Conclusions

A new TOA-based technique to accurately locate WLAN terminals has been presented. Since TOA is estimated at the link layer, this proposal requires only minor changes on the hardware of the IEEE 802.11 b card: adding a counter (including triggers to start and stop) and interfacing the triggers and the result of the counter to the software. Estimating the TOA at the link layer involves more error sources than if the estimation is done at the physical layer; this paper proposes statistical methods to overcome the impact of such errors. A Kalman-based filter is used to track the MT's trajectory using the previously obtained distances as observables. First results show positioning accuracies lower

than 0.9 m for the 66% of the cases.

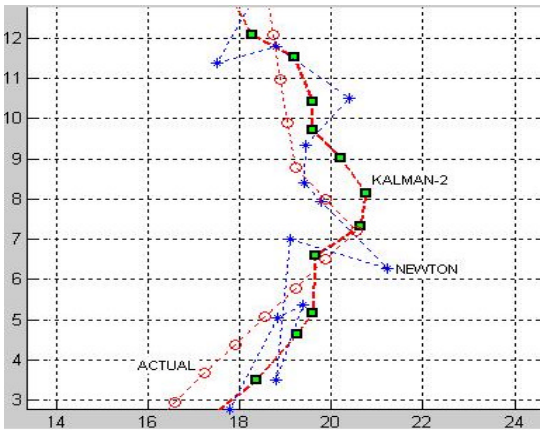

Figure 10. Actual and estimated trajectories

IV. OTHER TECHNOLOGIES

A. *Ultra Wide Band (UWB)*

The work on UWB-based positioning focused on the analysis of the potential ranging and positioning accuracy of future LDR UWB systems compliant to the IEEE 802.15.4a standard, currently under development.

The analysis took into account the characteristics of the UWB propagation channel (in terms of both communication range and impact on the ranging accuracy) as well as the Medium Access Control strategy to be adopted in the 802.15.4a standard, based on Aloha, and the impact of Multi User Interference.

Two different scenarios were selected for this analysis in order to represent the different application scenarios expected to be served by the new IEEE 802.15.4a standard. The first scenario was characterized by a centralized controller determining the position of fixed or mobile nodes based on the distance estimations provided by a set of fixed reference nodes. A Time Difference Of Arrival approach adopting a Least Square Error minimization was used for estimating the position of the terminals at the central controllers. An indoor environment characterized by both LOS and NLOS links was considered. Simulation results show that the positioning error is potentially very low in the case of LOS links between nodes, and remains acceptable even in presence of a significant percentage of NLOS links

The second scenario addressed the case when no external infrastructure is available, and relative position information must be built from scratch within the network. The scenario was characterized by a network of terminals that build a coordinate system exchanging distance and position information by means of a distributed algorithm derived from the Self Positioning Algorithm (SPA) [25].

In this case the selected performance indicators were the percent position error and the percentage of nodes that are able to converge to a single coordinate system, and can thus use and provide valid position information.

In this scenario the results indicated that, for a network with high enough terminal density, a distributed protocol combined with an IEEE 802.15.4a UWB physical layer can potentially provide accurate position information even in absence of any external infrastructure, despite the potentially high MUI interference caused by the strong signaling overhead in the construction of the common coordinate system required by the SPA algorithm.

Further investigation is now undergoing in a more detailed simulation scenario for emergency situations, taking into account: a) the impact of positioning the reference nodes outside of the building in the centralized scenario, causing thus a strong NLOS propagation and a potentially high Geometric Dilution Of Precision (GDOP), and b) the effect of a low terminal density and a high GDOP, which are to be expected in the typical emergency scenarios considered in the LIAISON project, in the distributed positioning case.

Further information on the results of UWB research activity within LIAISON can be found in [26], [27] and [28].

B. *Inertial Navigation Systems*

Inertial Navigation Systems (INS) are commonly used in the naval and aviation fields. While pedestrian navigation is based on the same underlying principles, i.e. measure of accelerations and angular velocities, the quality of the sensors employed differ from the “traditional” inertial systems. Due to constraints on ergonomics (weight and size), power consumption and price, the sensors used in pedestrian navigation are based on Micro-Electro-Mechanical Systems (MEMS) technology [20].

The Liaison research activities in this domain of MEMS based location focus on two primary axes:

- Research of algorithms for real-time implementation to detect and characterize human physical activities. In this context, human physical activity encompasses both body postures (lying, sitting and standing) and body displacement (distance travelled and azimuth of travel).
- Coupling of MEMS derived body displacement with absolute positioning information provided by other technologies, such as Assisted GNSS (A-GNSS) or wireless location.

With respect to the first point, a novel approach in the context of pedestrian navigation is being pursued that consists on placing sensors in different parts of the human body, specifically the trunk, thigh and shank. With this architecture it is possible to determine the real posture of a pedestrian. This information is not only useful to infer about his safety condition, but also to adjust the navigation algorithms to certain specific movements of the professional users (e.g. crawling or walking squatted) [21].

As a first step in the procedure of validating this approach, a few tests have been performed under less stringent conditions, both in terms of movement complexity (postures and displacement) and environmental conditions. The results obtained show a rate of success of better than 95% in posture

detection and 90% in detecting the type of displacement (forward, backward, lateral movement, stairs climbing and descending). As for the quantification of the actual displacement, the errors observed are less than 5% of the distance travelled and 1 degree in orientation (in magnetically free environments) [21]. Validation of these results under more severe conditions is planned for the near future.

Future research activities on this axis will contemplate the following points:

- Adaptation to the project's test cases specific movements and context: the aim is to further improve the various algorithms to obtain a better performance under more stringent conditions.
- Online calibration: one of the main challenges in pedestrian navigation based on MEMS is to reduce the effect of large bias and noise levels typical of these sensors. The use of calibration phases is a good methodology to reduce the errors. It is possible to do an a priori calibration or an online calibration. The first consists of using a known reference to correct the processing results of the MEMS signals. Previous EPFL research on the Pedestrian Navigation Module [22] has proven this solution. Our intention is to work in addition with the online calibration. This procedure intends to benefit from external outputs or identified postures to correct the sensors errors.

Regarding the second research axis pursued under Liaison, work is currently undergoing to hybridize MEMS based positioning with other positioning technologies, namely A-GNSS and WiFi TOA/Fingerprinting. Besides increased availability of the overall system, this approach allows the correction of certain systematic errors on the MEMS side (i.e. step length and orientation errors), improving positioning accuracy [23][24].

V. Conclusion

Indoor location with WiFi allows using the existing infrastructure and devices widely deployed in buildings such as airports, train stations, hotels, etc. The two approaches presented in this paper provide a good accuracy. UWB (in ad hoc mode) and INS can be used in extreme cases such as fire when infrastructure is disconnected.

References

[1] X. Li; K. Pahlavan, M. Latva-aho, M. Ylianttila, "Comparison of Indoor Geolocation Methods in DSSS and OFDM Wireless LAN Systems", *IEEE VTS-Fall VTC 2000*. 52nd, Volume 6, 24-28 Sept. 2000, pp. 3015-3020.

[2] D. McCrady, L. Doyle, H. Forstrom, T. Dempsey, M. Martorana, "Mobile Ranging Using Low-accuracy Clocks", *IEEE Transactions on Microwave Theory and Techniques*, Volume 48, Issue 6, June 2000, pp.951-958.

[3] A. Günther, C. Hoene, "Measuring Round Trip Times to Determine the Distance Between WLAN Nodes", *Networking 2005*, pp. 768-779

[4] A. M. Ladd, K. E. Bekris, A. P. Rudys, D. S. Wallach, and L. E. Kavraki, "On the Feasibility of Using Wireless Ethernet for Indoor Localization", *IEEE Transactions On Robotics And Automation*, Vol. 20, No. 3, pp.555-559, June 2004.

[5] H. Hashemi, "The Indoor Radio Propagation Channel", *Proceedings of the IEEE*, Vol. 81, No.7, July 1993, pp. 943-968.

[6] R. Kalman, "A new approach to linear filtering and prediction problems", Trans. ASME, J. Basic Eng. 82D, pp. 35--45, 1960.

[7] G. Welch and G. Bishop. "An introduction to the kalman filter". Technical Report TR 95-041, University of North Carolina at Chapel Hill, 1995

[8] A; Motley and J. Keenan, "Personal communication radio coverage in buildings at 900 MHz and 1700 MHz", Electronics Letter, vol. 24, June 1988

[9] R. Vaughan and J. B. Andersen, Channels, propagation and antennas for mobile communications. Electromagnetic Waves Series 50, The IEE, London, United Kingdom, 2003

[10] A. Smailagic and D. Kogan, "Location sensing and privacy in a context-aware computing environment", IEEE Wireless Communications, Oct. 2003

[11] P. Bahl and V. Padmanabhan, "RADAR: an in-building RF-based user location and tracking system", Proceedings IEEE Infocom 2000, Tel Aviv, Israel, col. 2, pp. 775-784, Mar. 2000.

[12] R. Battiti, T. L. Nhat and A. Villani, "Location-aware computing: a neural network model for determining location in wireless LANSs", tech. rep, Dept. of Information and Communication Technology, Univ. of Trento, Feb. 2002

[13] A. Hatami and K. Pahlavan, "A comparative performance evaluation of RSS-based positioning algorithms used in WLAN networks", IEEE Wireless Communications and Networking Conference, 2005

[14] T. Roos, P. Myllymäki and J. Sievänen, "A probabilistic approach to WLAN user location estimation", International Journal of Wireless information Networks, vol. 9, July 2002

[15] T. Roos, P. Myllymäki and H. Tirri, "A statistical modeling approach to location estimation", IEEE transactions on Mobile Computing, vol. 1, Jan. 2002

[16] L. Liao, D. Fox, J. Hightower, H. Krautz, D. Schultz, "Voronoi tracking: location estimation using sparse and noisy sensor data", Proc. Of the International Conference on Intelligent Robots and Systems (IROS, IEEE/RSJ, 2003.

[17] S. Arulampalam, S. Maskell, N. Gordon, T. Clapp, "A tutorial on particle filter for on-line non-linear/nongaussian Bayesian tracking", IEEE transactions on Signal Processing, vol. 50, no. 2, Feb. 2002

[18] LIAISON, Deliverable 27 (D027)

[19] S. Arulampalam, S. Maskell, N. Gordon and T. Clapp, "A tutorial on particle filters for on-line non-linear/nongaussian bayesian tracking", IEEE Transactions on Signal Processing, vol. 50, Feb. 2002

[20] Q. Ladetto and B. Merminod, "In Step with INS – Nvaigation for the Blind, Tracking Emergency Crews", in GPS World, October 2002.

[21] LIAISON, Deliverable 54 (D054).

[22] Q. Ladetto, "Capteurs et algorithmes pour la localisation autonome en mode pédestre", in ENAC INTER TOPO, 2002, Ecole Polytechnique Fédérale de Lausanne.

[23] Q. Ladetto, "On foot navigation : continuous step calibration using both complementary recursive prediction and adaptive Kalman filtering", in ION GPS 2000, 2000, Salt Lake City.

[24] Q. Ladetto et al., "Human Walking Analysis Assisted by DGPS", in GNSS 2000, Edinburgh.

[25] S. Capkun, M. Hamdi and J. P. Hubaux, "GPS-free positioning in mobile Ad-Hoc networks," Hawaii International Conference On System Sciences, HICSS-34 January 3-6, 2001 Outrigger Wailea Resort, pp. 3481 - 3490.

[26] R. Cardinali, L. De Nardis, P. Lombardo and M.-G. Di Benedetto, "UWB Ranging Accuracy in High and Low Data Rate Applications," Special Issue on UWB, IEEE Transactions on Microwave Theory and Techniques, Volume 54, Issue 4, April 2006, pp. 1865 - 1875.

[27] L. De Nardis and M.-G. Di Benedetto, "Positioning accuracy in Ultra Wide Band Low Data Rate networks of uncoordinated terminals," accepted for the IEEE International Conference on UWB 2006 (ICUWB 2006), September 2006, Boston, USA.

[28] LIAISON Project, Deliverable D054 "Solution Research Results Data Package [Iss. 02]," July 2006.